

Research paper

# Introducing a tailored site delineation approach to optimize the design of managed aquifer recharge surface spreading infrastructure

Rebecca Sultana<sup>a,b,\*</sup>, Ulrike Werban<sup>b</sup>, Marco Pohle<sup>b</sup>, Thomas Vienken<sup>c,b</sup>

<sup>a</sup> Technical University of Munich, TUM Campus Straubing for Biotechnology and Sustainability, Am Essigberg 3, 94315, Straubing, Germany

<sup>b</sup> UFZ-Helmholtz Centre for Environmental Research, Permoserstrasse 15, 04318, Leipzig, Germany

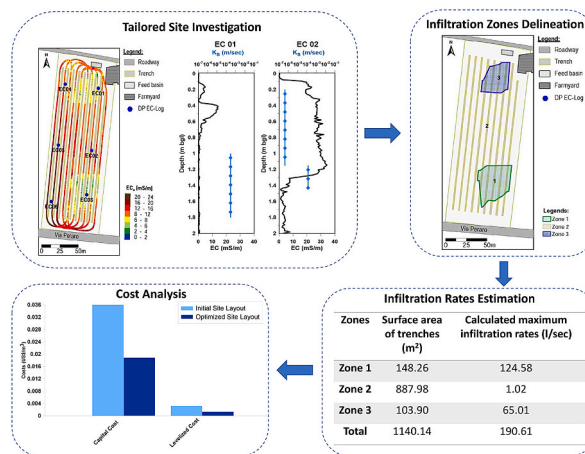
<sup>c</sup> Weihenstephan-Triesdorf University of Applied Sciences, TUM Campus Straubing for Biotechnology and Sustainability, Am Essigberg 3, 94315, Straubing, Germany



## HIGHLIGHTS

- A novel approach for optimized MAR design by combining site exploration, infiltration rate estimation, and cost analysis.
- Identification of lateral and vertical variation of subsurface.
- Delineation of potential infiltration zones resulting in 77.9% land use reduction.
- Reduction of cost per cubic meter of recharged water by 59.1% compared to the initial cost.

## GRAPHICAL ABSTRACT



## ARTICLE INFO

## Keywords:

Managed aquifer recharge  
Infiltration prediction  
Site exploration  
Cost analysis

## ABSTRACT

Managed aquifer recharge (MAR) is an emerging solution to effectively replenish overused groundwater resources, but high associated costs often hinder its uptake. There are several parameters to consider when determining the cost of MAR, including recharge types, scale of MAR schemes, land acquisition, operation and maintenance period, and the hydrogeological setting. Hydraulic conductivity and its spatial variability are the most significant hydrogeological parameters for predicting infiltration rates at MAR sites, but limited data availability makes accurate predictions often challenging. Hence, it is essential to increase data availability to optimize MAR efficiency and to better assess its economic performance. Therefore, a novel approach for MAR planning is presented in this article to efficiently enhance the data availability during the conceptual stage of MAR planning by combining site exploration, spatially resolved infiltration rate estimation, and cost analysis. The approach was applied at an actual MAR site in Vincenza, Italy, and incorporated an electromagnetic induction survey and direct push profiling as across-scale investigation methods to enhance site delineation and

\* Corresponding author. Technical University of Munich, TUM Campus Straubing for Biotechnology and Sustainability, Am Essigberg 3, 94315, Straubing, Germany.

E-mail address: [rebecca.sultana@tum.de](mailto:rebecca.sultana@tum.de) (R. Sultana).

<https://doi.org/10.1016/j.gsd.2024.101169>

Received 16 June 2023; Received in revised form 10 March 2024; Accepted 1 April 2024

Available online 5 April 2024

2352-801X/© 2024 The Authors. Published by Elsevier B.V. This is an open access article under the CC BY license (<http://creativecommons.org/licenses/by/4.0/>).

subsequent parameterization of the identified zones using laboratory analysis of collected samples. This MAR site is particularly suitable for its heterogeneous subsurface structure and potential to counteract groundwater depletion. The performed investigation resulted in an image of the lateral variation of subsurface conditions and allowed the delineation of three zones with different infiltration behavior, with 99.5% of infiltration occurring in just two zones, representing only 22.1% of the site. In this particular scenario, the overall cost per cubic meter of recharged water can be reduced by 59.1% by identifying and eliminating unfavorable zones. This study provides scientists and practitioners with a useful tool for MAR planning that can be applied to a wide range of sites with complex geology, thereby reducing water costs, minimizing the environmental impact of infrastructure construction, and reducing land use conflicts.

## 1. Introduction

Groundwater is an important water resource on which two billion people worldwide rely for drinking (Morris et al., 2003). Globally, it provides over 40% of irrigation water (Ross, 2016). Several agricultural regions have seen significant poverty reduction and economic growth with the start of intensive groundwater extraction, along with improving food security and drought management (Giordano and Villholth 2007; Giordano 2009). Nevertheless, the world's water supply is threatened by population growth, agricultural intensification, industrialization, and global warming (Hossain et al., 2021). The overexploitation of groundwater will reduce water availability for domestic, agricultural, and industrial purposes, thus threatening local economies and the social well-being of the local community. Groundwater problems do not only have sectoral, state, or national borders but also involve human interests (Jakeman et al., 2016).

Managed aquifer recharge (MAR) is an effective approach to replenish overexploited groundwater resources in stressed aquifers. This technique involves intentionally recharging aquifers from different sources, e.g., surface water, rainwater, storm runoff, or treated effluent (Bouwer, 2002; Dillon et al., 2009; Gale et al., 2002) and to be retrieved when water demand is high or supply is insufficient. MAR has the potential to sustain the availability of water supplies, overcome climate change impacts, and improve groundwater quality and quantity (Casanova et al., 2016). A wide range of MAR techniques such as surface spreading methods, river bank filtration, well injection, rainwater harvesting, and in-channel modifications (Sprenger et al., 2017) is applied in Europe for recharging aquifers on different scales. The choice of MAR type is thereby based on local conditions.

A number of significant benefits and demonstrated advantages have been associated with MAR, however its uptake has been below its potential (Ross and Hasnain, 2018). The global uptake of MAR is largely determined by its financial and economic characteristics (Maliva, 2014). Most often, a water project's economic assessment aims to evaluate whether its benefits outweigh predicted costs or to compare alternative approaches (Halysia et al., 2022). This is especially important as the finances allocated to water projects are often limited, and they have to compete with other equally important projects such as health, and transportation (Maliva 2014). In addition, MAR infrastructure is often built in sensitive ecosystems or competes with other land use purposes, such as agriculture. Hence, costs of MAR, and costs per cubic meter ( $\text{m}^3$ ) of recharged water are determined by capital, operational, and maintenance (O&M) expenditures. These expenditures are again impacted by a wide variety of hydrogeological, socio-economic, legal, and institutional factors (ASR Systems 2006; Dillon et al., 2009). Understanding these is critical to the technical, economic, and ecological optimization of MAR system design and performance. The primary technical parameter to predict infiltration rates at MAR sites is hydraulic conductivity and knowledge about its spatial variability (Barquero et al., 2019). Different studies have demonstrated spatial variations in infiltration rates due to subsurface heterogeneity (Becker et al., 2013; Mawer et al., 2016; Medina et al., 2020; Racz et al., 2012) in this regard. However, spatially resolved predictions of infiltration rates, ideally in the planning phase, are challenging to obtain, as measurements are often not able to

accurately characterize spatial heterogeneity of sedimentary deposits encountered at MAR sites. The limited data availability is a frequent cause of MAR site failure or poor performance (Maliva et al., 2006; Naik et al., 2017). In this article, we demonstrate how MAR planning can be optimized by enhancing data availability in the conceptual MAR planning phase through the application of an adaptive site characterization with across-scale exploration methods. As part of this study, a concrete MAR site located near an agricultural area in the Schiavon municipality in Vicenza, Veneto, Italy, was investigated. The heterogeneous subsurface structures make the alluvial aquifer an interesting study. While years ago, e.g. during the planning of the investigated MAR site, the applied techniques were beyond state of the art, the innovative characterization approach has proven its feasibility for complex hydrogeological site investigation in academia and practice over the last decade (Utom et al., 2019; Vienken et al., 2012; Vienken et al., 2017). We used and combined subsurface characterization methods to identify zones of varying soil properties across the site and estimated the infiltration rate variation between the zones. Lastly, an assessment of the capital and operation cost of the MAR site was performed which allows a tailored MAR design and planning. The developed approach aims to be transferable to other MAR sites because an optimized MAR design will reduce the cost of water, the environmental footprint of the built infrastructures, and land use conflicts. It will therefore contribute to the uptake of MAR in times of accelerating water demand.

## 2. Materials and methods

In the following, we provide an overview of the investigated MAR site and explain the site characterization approach, which involves the combined application of geophysical methods, direct push (DP) profiling, and core sampling. After that, we explain the chosen approach to calculate infiltration rates depending on the infiltration trench geometry, water depth in the trench and saturated hydraulic conductivity ( $K_s$ ) and, lastly, illustrate the economic assessment of the MAR site.

### 2.1. Study area

The Schiavon Forested Infiltration Area (FIA) site was installed in 2009 to alleviate groundwater scarcity in the Vicenza upper plain aquifer of the Brenta megafan, an unconfined aquifer of the pre-Alpine region (Mastrocicco et al., 2015; Piccinini et al., 2016). In recent years, over-exploitation of groundwater, climate change, and land use have caused the overall reduction of water levels in this aquifer of the Brenta megafan, thus reducing the water availability for agricultural, industrial, and collective use. The site covers an area of 1.1 ha, applying furrow irrigation to recharge the unconfined aquifer. A channel feeds the system, which is connected to local canals that divert water from the Brenta River for irrigation (Mastrocicco et al., 2015). It comprises nine infiltration trenches with a distance of 7.5 m between the trenches. Each trench has a trapezoidal cross-section (0.7–0.8 m top width and 0.3–0.4 m bottom width) with a length of 163 m which sums up to a total length of 1467 m. The trenches are 0.7–0.8 m deep (Filippi et al., 2016), and the surface water is distributed among the infiltration channels by a level control system (Sottani et al., 2014) to recharge the groundwater at

about 19 m below the ground surface (Mastrocicco et al., 2015). At this infiltration site, trees and shrubs (1400 plants/ha) are planted between the trenches in five years of short rotation forestry to reduce water evaporation and produce additional biomass to buffer land costs and subsequently reduce the costs of the recharged water.

Mastrocicco et al. (2015) provided an overview of the surface-near site stratigraphy. Three horizons were identified: The topsoil extends, from 0 to 0.35 m below ground level (bgl), and shows the influence of tillage and plant root growth and has a sandy loamy structure with a 20% gravel skeleton. The middle horizon (0.35–0.75 m) comprises two layers. The upper part (0.35–0.45 m) has a sandy clay loam texture, abundant coarse gravel skeleton (55%), and frequent clay coatings, indicative of clay adhering to the surfaces of both gravel particles and soil aggregates. In the lower part (0.45–0.75 m) the texture transitions to sandy loam, accompanied by 55% gravel skeleton and fewer clay coatings. The lower horizon extends to 1.2 m bgl has a sandy texture with 60% coarse gravel skeleton. The  $K_s$  at these horizons was determined by a Guelph Permeameter and varied over several orders of magnitude between  $6.6 \times 10^{-05}$  m/s and  $1.7 \times 10^{-02}$  m/s, see Mastrocicco et al. (2015). This broad range shows the relevance of proper knowledge of subsurface conditions for better MAR design and planning within the heterogeneous deposits of the Brenta River megafan.

## 2.2. Site investigation

Conventional approaches for hydrogeological high-resolution site characterization to identify variations in hydraulic conductivity and, subsequently, potential variations in infiltration rates across entire sites are often expensive and time-consuming. Hence, data collection is restricted to point measurements at few selected locations which may fail to provide representative information regarding the variability of subsurface properties (Binley et al., 2015; Kalbus et al., 2006). Thus, numerical models often need to simplify or up-scale heterogeneity as insufficient data are available to reliably represent subsurface heterogeneity (De Marsily et al., 2005; Koltermann and Gorelick, 1996) on a larger scale making accurate prediction of MAR scheme performance difficult. Our site investigation aimed to characterize the subsurface properties of the infiltration site and to map variability in sediment properties. The applied methodological approach incorporated electromagnetic induction surveying (EMI), direct push (DP) electrical conductivity (EC) profiling, DP-based soil sampling, and laboratory analysis of collected samples.

The first step of the site investigation was to use non-invasive and rapid EMI measurements to screen for any potential spatial variability of the subsurface at shallow depths. EMI is a method of determining the soil apparent electrical conductivity ( $EC_a$ ), which represents the bulk EC for a volume of soil under investigation (Martini et al., 2017). Because of its non-invasive nature and fast operation, EMI surveys are ideal for measurements of lateral variation in soil properties at spatial scales (von Suchodoletz et al., 2022).

With the EMI we focused on delineating the spatial variability of soil  $EC_a$  as under non-saline conditions, an increase in soil EC often correlates with the increased abundance of clay minerals (Vitharana et al., 2006). The increased abundance of fines may, in turn, strongly hinder infiltration and lead to locally reduced infiltration rates. By employing the EMI as a screening method, we intended to enhance the MAR planning process while simultaneously reducing the costs associated with detailed mapping. After distinguishing areas of interest, we selected representative locations to perform minimally invasive DP EC logging and soil sampling to obtain vertical high-resolution profiles of relevant subsurface properties over depth. Lastly, obtained soil samples were used to determine  $K_s$  on selected samples as a basis for calculating infiltration rates.

### 2.2.1. EMI measurements

Electromagnetic instruments typically comprise transmitter and

receiver coils (McNeill, 1980). The transmitter coil generates a primary electromagnetic field at a specific frequency. This field induces eddy currents in conductive materials in the subsurface, generating a secondary magnetic field detected by the receiver coil. The receiver coil detects the induced secondary and primary fields to estimate  $EC_a$  (Doolittle and Brevik, 2014). EMI surveys were conducted with an EM38DD electromagnetic induction sensor (Geonics Ltd., ON, Canada) containing two transmitter and receiver coils with a fixed spacing of 1 m. The simultaneous measurement of  $EC_a$  is performed in two orientations with different depth response profiles. The horizontally oriented sensors receive the response from the uppermost 0.75 m of the soil. The effective depth of investigation using the vertical dipole mode is up to 1.5 m (Callegary et al., 2012; McNeill, 1980). In this investigation step, we focused on the vertical dipole measurements to obtain data across the infiltration trench depth and deeper. Ten parallel profiles between the infiltration trenches were measured (Fig. 1) with a sampling interval of 0.2 sec. Positioning was performed with a differential GPS (smart antenna A100, Hemisphere GNSS). After aerial information was collected, DP EC logging locations were chosen to obtain further information about the vertical distribution of EC at the selected points.

### 2.2.2. DP EC logging and soil sampling

During DP probing, small-diameter hollow steel rods are driven, pushed, and/or vibrated into the subsurface (EPA, 1997). A variety of sensor probes can be attached to the rod string end to enable high-resolution continuous in-situ measurements of hydrogeological, hydrological, geophysical, geochemical, or geotechnical data in un- or weakly consolidated sedimentary deposits (Dietrich and Leven 2006). DP EC logging has proven particularly effective in investigating sediment properties variation (Schulmeister et al., 2003). It has a number of advantages over many traditional site investigation approaches. These include the measurement of vertical high-resolution depth-accurate in-situ information of hydrogeological and petrophysical sediment properties, its minimally invasive characteristics, as well as lower expenses, higher speed and improved field accessibility (Butler 2002; Dietrich and Leven 2006). The DP EC probe has four point electrodes at the side of the probe with 0.02 m electrode spacing. Resistivity measurements are made via the 0.065 m long electrode array at every 0.015 m depth increase and provided as EC. Furthermore, the DP EC system provides EC in contrast to the EMI ( $EC_a$  output) because it records EC and depth values simultaneously. The support volume of the individual DP EC is considerably low due to the small electrode array. Depth resolved EC measurements are especially helpful in the context of MAR site investigation to delineate the presence of even thin confining layers that may impede water percolation through the unsaturated zone and, hence, groundwater recharge.

Six DP EC probing points were chosen based on the EMI survey results (Fig. 1). Based on the EC logging results, soil samples using 1.2 m long and 3 cm diameter plastic tube liners were collected for further laboratory analysis. 15 individual soil samples at four locations were obtained at locations EC 01, EC 02, EC 03, and EC 05 (Fig. 1).

### 2.2.3. Laboratory analysis of sampling material

Soil samples obtained at selected points were used to i) determine the grain size composition, especially the abundance of the silt and clay fraction; and ii) measure  $K_s$  using a constant head permeameter, KSAT device (METER Group AG, 2016) for 250 cm<sup>3</sup> samples to estimate infiltration rates. The measurement range of the KSAT device is  $1.16 \times 10^{-09}$  m/s to  $5.79 \times 10^{-04}$  m/s. The infiltration rate was estimated with the following equation used for a canal with a deep ground water table in an isotropic homogeneous porous medium (Swamee et al., 2000)-

$$q_i = K_s F_t \quad (1)$$

where,  $q_i$  = the infiltration rate per unit length of the trench (m<sup>2</sup>/s), and  $F_t$  = the seepage function dependent on the geometry of the trench

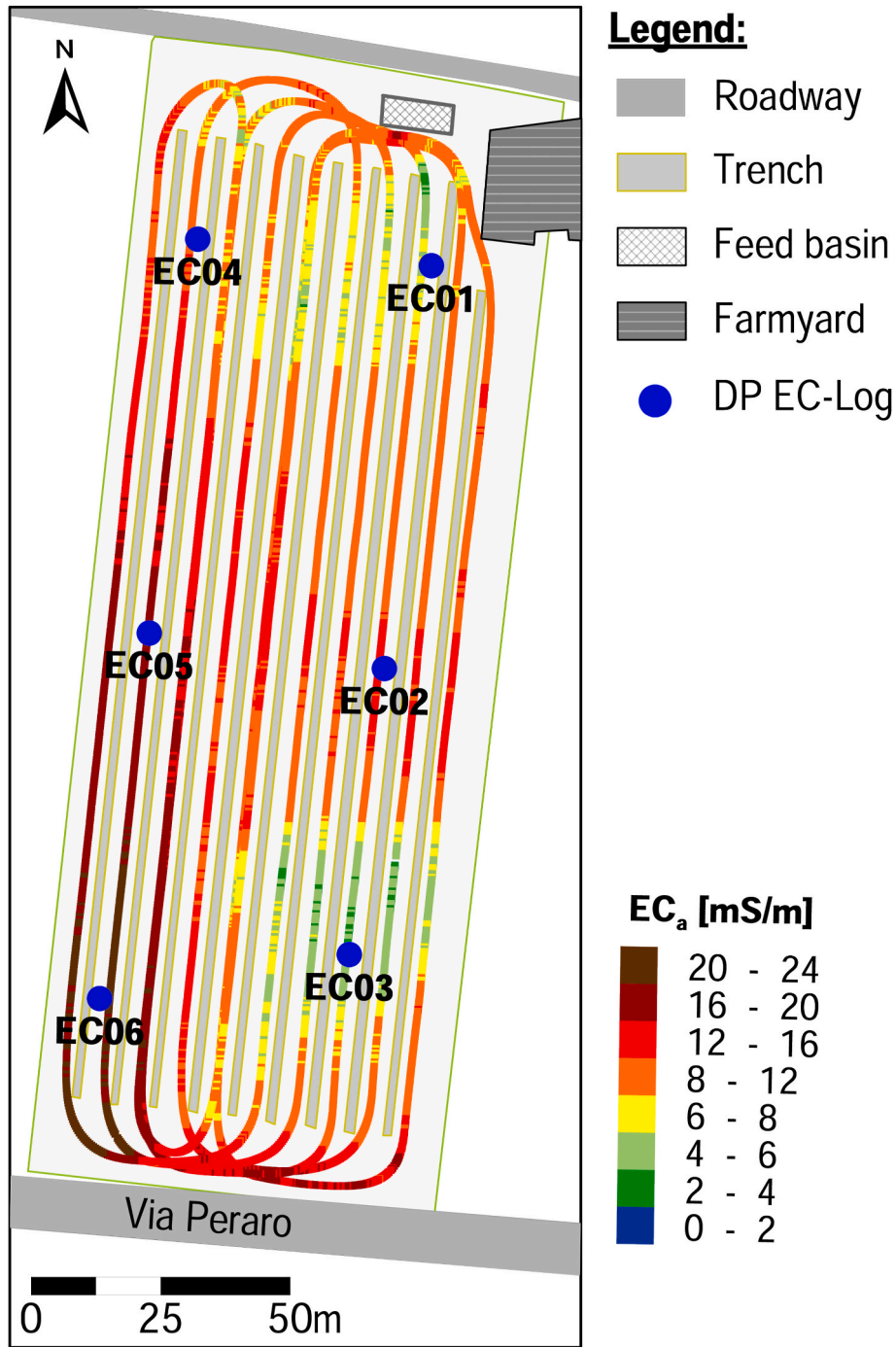


Fig. 1. Results of the EMI survey, EM38DD with 1.5 m penetration depth and location of six DP EC logging points.

(dimensionless).

For a trapezoidal channel, the seepage function ( $F_t$ ) can be expressed as-

$$F_t = \left[ \{ (4\pi - \pi^2)^{1.3} + (2m)^{1.3} \} \frac{0.77+0.462m}{1.3+0.6m} + \left( \frac{b_w}{y_w} \right)^{\frac{1+0.6m}{1.3+0.6m}} \right]^{\frac{1.3+0.6m}{1+0.6m}} \quad (2)$$

where,  $m$  = the side slope of the trench;  $b_w$  = the trench bottom width (m) and  $y_w$  = water level in the trench (m).

### 2.3. Cost analysis of Schiavon FIA

There are various types of costs associated with MAR projects: cap-

ital, operations and maintenance (O&M). Capital costs refer to the initial, non-recurring expenses associated with developing and building



the MAR system, encompassing various expenditures such as land procurement, feasibility assessments, testing, consultation services, construction expenses, and regulatory approval requirements during both construction and operational stages (Maliva, 2014). O&M costs are the expenditures required to maintain and operate a MAR system (Maréchal et al., 2020).

As described in Ross and Hasnain (2018), levelized cost estimates are typically employed for estimating MAR scheme costs. In the case of a water supply project, the levelized cost is expressed as the constant annual revenue required to recover all capital, O&M costs over the project's estimated lifetime divided by the annual volume of water supply. Levelized costs are a useful tool for comparing the water costs from MAR schemes and alternative water projects (Dillon et al., 2009).

To standardize the declared capital cost and O&M cost of the Schiavon FIA project, they were multiplied by a gross domestic product (GDP) deflator which tracks price changes of all goods and services produced domestically, to express costs in local currency units (LCUs) valued at the year 2022. The index values were obtained from the Organization for Economic Co-operation and Development (OECD, 2022). Afterward, capital and O&M costs in LCUs were converted to US dollars (US\$) for standardization based on the information from the European central bank (0.94 euros/US\$). According to Treasury (2003), a reduced discount rate of 3.5% is proposed for projects or investments between 0 and 30 years. MAR scheme operation life of 30 years and a discount rate of 3.5% were assumed for this estimation. The levelized cost estimation was based on the estimated infiltration rates for 200 operational days, considering the low flow and diversion of water for agriculture. More details regarding the levelized cost estimation of MAR schemes are provided by Ross (2022) and Ross and Hasnain (2018).

### 3. Results

#### 3.1. Spatial variation of soil $EC_a$ in EMI survey

The spatial mapping obtained by EM38DD exhibits a zonation of the soil  $EC_a$  across the test site which can be an indicator of distinct variations in soil properties. The  $EC_a$  measured at the site varies from 2.4 to 24 mS/m as presented in Fig. 1.

Three zones can be identified: 1) An isolated area with low to moderate  $EC_a$  values in the north of the test site; 2) an isolated area with low to moderate  $EC_a$  values in the south-east of the test site and 3) the rest of the area revealing higher  $EC_a$  values than the isolated area. An increase in  $EC_a$  is expected to correlate with an increase in clay mineral

content, leading to lower hydraulic conductivity and hence, reduced recharge rates.

The lateral variation in soil properties can be effectively delineated by the EMI survey at the site. However, the determined  $EC_a$  is a bulk conductivity measurement over a soil volume to a particular depth, in this case, 1.5 m. Hence, DP EC logging was applied in the identified zones to obtain in situ high-resolution information about vertical EC variation.

#### 3.2. Investigating vertical heterogeneity with DP EC logging profiles

Fig. 2 shows the vertical high-resolution EC logging profiles from the six locations (EC 01 to EC 06) that were positioned to reflect the different EMI zonation and to represent the site. The main finding of the EMI survey is supported by the DP profiling, as generally low EC values in the upper 1.5 m bgl are encountered at probing locations EC 01 and EC 03 that were positioned in the isolated zones of low soil  $EC_a$ . The most relevant individual features identified in the logging profiles are described in the following.

Profile EC 01 differs from all other logging profiles. EC values are very low in the profile except for two horizons with higher values between 0.4 and 0.6 m bgl and beginning at 8.20 m bgl. At EC 02, there is a distinct layer present up to 1.25 m bgl with increased EC values. It is important to note, that this distinct area of increased EC values, indicating a higher clay mineral content, is below the base of the trenches. EC 03 does not feature a surface-near zone of increased EC values. In contrast, an isolated interval with high EC values of up to 100 mS/m appears at a depth of 5–6 m bgl, which indicates the strong presence of clay minerals. Recorded values at EC 04 and EC 05 again exhibit increased EC values in the upper 1.8 m bgl. The logging profile measured at EC 06 indicates generally low EC values and only minor vertical variation, with the exception of a small isolated EC peak at 2.24 m bgl.

The DP EC logging results reveal a significant variation in measured EC values underlining the high degree of subsurface variability at the site. A strong lateral variation between the logs can be identified, which is reflected in the discontinuity of most of the isolated features indicating clayey lenses, especially at greater depths. Because of their discontinuity, the lenses of increased EC do not affect the overall infiltration rate at the site. However, this is different for the surface near high EC zones, as their bases are below the trench bottom levels and directly hinder infiltration in these areas. Further information was needed to quantify the effects of surface-near variation in EC values on the infiltration rates. Thus, soil samples were obtained to compare grain

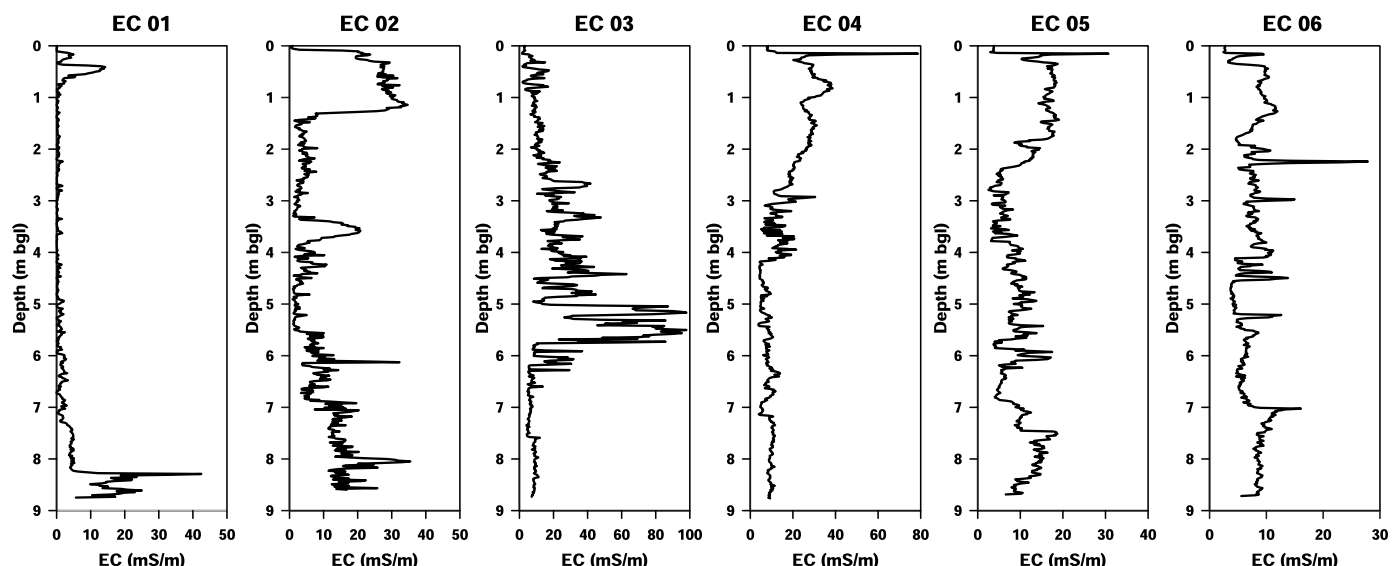


Fig. 2. Vertical variation in EC at six DP EC logging profiles up to 9 m depth bgl. Please note the individual scaling of x-axes.

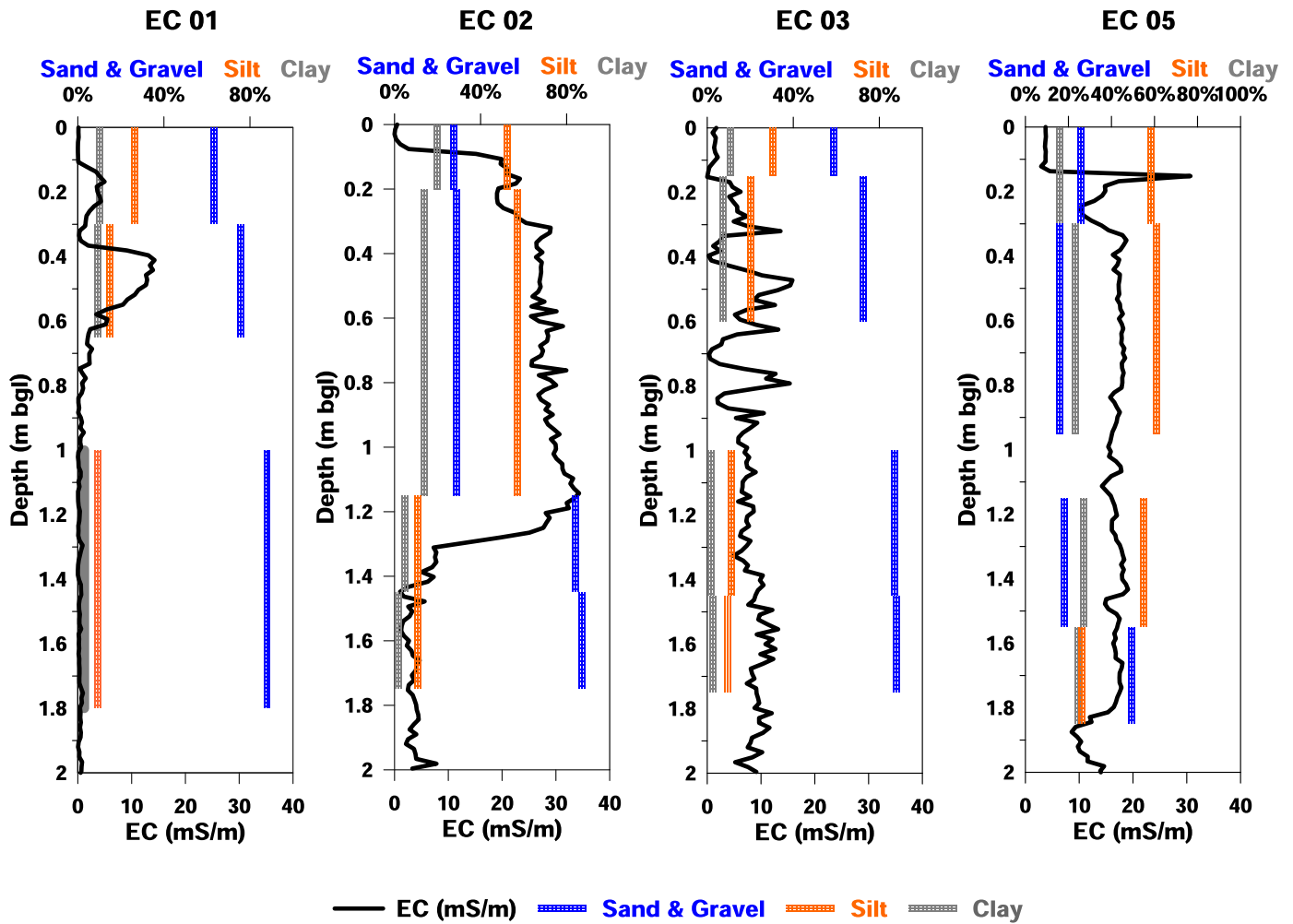


Fig. 3. Combined representation of DP EC profiles and percentage of sand and gravel, silt, and clay at four probing points up to 2 m bgl.

size distribution to the EC values, and, in a second step measure  $K_s$  to determine infiltration rates at selected probing points.

### 3.3. Comparison of DP EC data to grain size analysis and $K_s$

Results of the grain size analysis are provided in Fig. 3 and Table S1. Results at EC 02 show the abundance of fine materials in intervals with increased EC. This can be recognized at EC 02 where high percentages of clay (14%) and silt (57%) at 0.2–1.15 m bgl match increased EC values. At EC 05, EC values of approximately 15 mS/m are measured with only minor variation between 0.35 and 1.8 m bgl. An increased share of clay in the sediment samples is present in the same depth interval, ranging between 23% and 27% of the sampled material. It is interesting to note, that the amount of clay found at EC 05 leads to measured EC values of 15 mS/m while half the amount of clay content (14%) over the depth interval of 0.2–1.15 m bgl leads to a much higher EC of around 30 mS/m at EC 02.

DP EC results are reliable indicators for detecting relative changes in fine-grain content in this study despite single isolated discrepancies between DP-measured EC and the results of the grain size analyses (see discussion section for further information). Hence, we used the DP EC data to identify 8 sampling intervals. Direct measurements of  $K_s$  were chosen, as  $K_s$  depends on a number of factors other than grain size composition, such as packing density, porosity, and tortuosity (Vienken and Dietrich, 2011). Three  $K_s$  measurements were performed for each soil sample and the arithmetic mean of the values was taken to represent  $K_s$  of each soil sample. Fig. 4 indicates the sampling intervals and

compares the vertical variation of EC and  $K_s$  at four DP EC locations.

The determined  $K_s$  values range over three orders of magnitude between  $4.26 \times 10^{-07}$  m/s and  $3.67 \times 10^{-04}$  m/s (Table S2). At EC 01,  $K_s$  at 1–1.8 m bgl was high ( $2.73 \times 10^{-04}$  m/s) which indicated the presence of sand and gravel dominated deposits, while comparably higher EC values of 13.63–34.31 mS/m between 0.2 and 1.15 m bgl are reflected by a comparably lower  $K_s$  value of  $4.26 \times 10^{-07}$  m/s at EC 02. It is important to note that the low EC values obtained at EC 01 are primarily caused by an insufficient electrical coupling of the probe to the ground, indicating dry, non-cohesive sediments (see discussion for further information). Grain size analysis and measured  $K_s$  results demonstrate that the subsurface properties are varying at different points and over depth.

### 3.4. Delineation of different zones and infiltration rates

The eventual step in this research was to distinguish zones with different infiltration behavior and to determine specific infiltration rates. The infiltration site was categorized into three different zones based on the obtained results (Fig. 5).

Infiltration rates were calculated for three zones based on the  $K_s$  using equation (1). Information about average water level depths in the trenches was not available. Hence, an average water level of 0.4 m was assumed for estimating the infiltration rates in the trenches. The estimated infiltration rates based on the total length of the infiltration trenches in the three zones are represented in Table 1.

The total maximum infiltration rate at the site is 190.61 l/s,

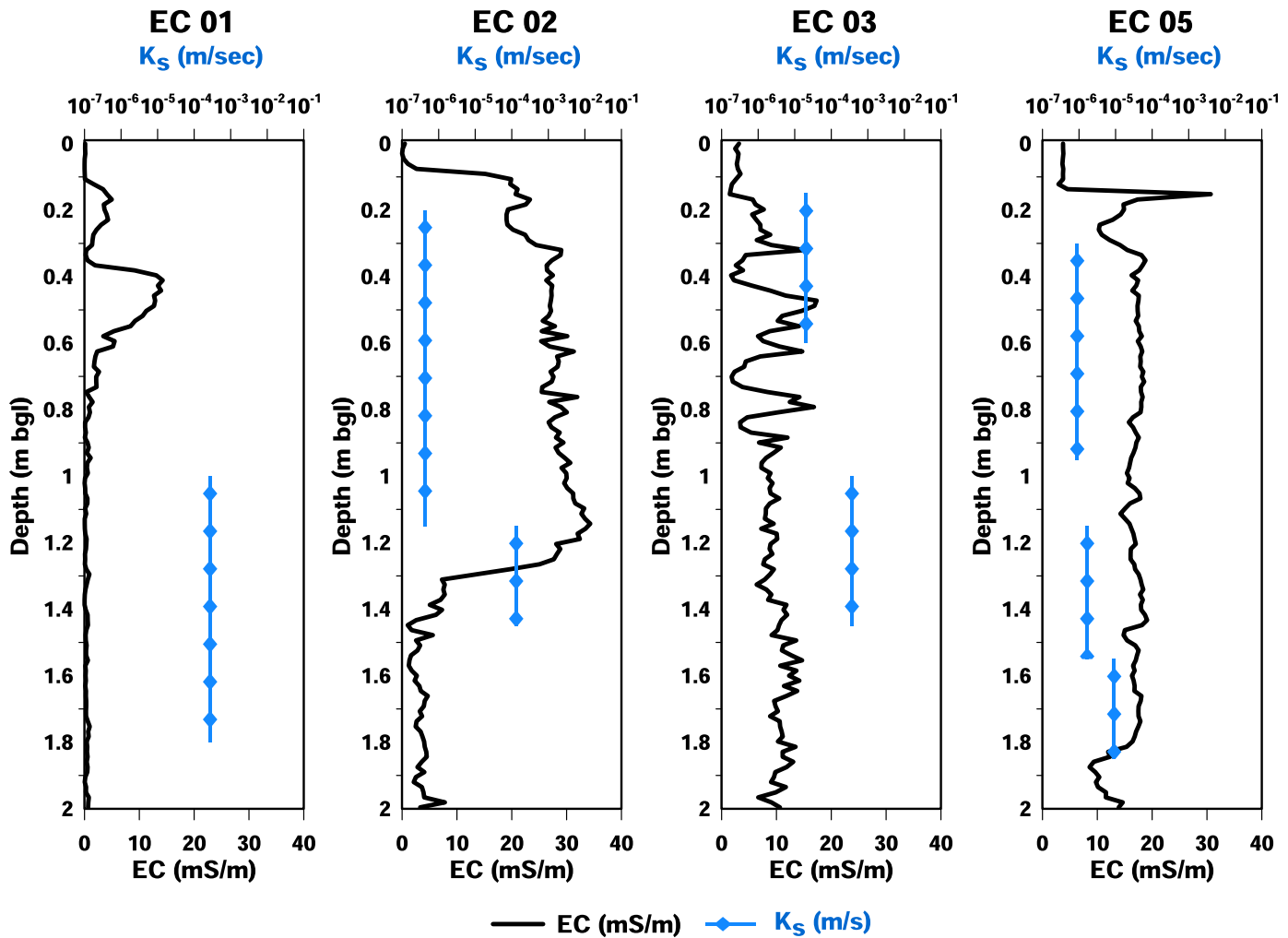


Fig. 4. DP EC logging profiles and sample based  $K_s$  measurements at four DP EC logging points up to 2 m depth bgl.

considering the trenches are continuously filled to a height of 0.4 m from the trench bottom. Substantial differences in calculated infiltration rates can be observed between the individual infiltration rates at each zone, see Table 1. Zone 1 can infiltrate 124.58 l/s of surface water, which is the highest among all the zones. The lowest amount of recharge with 1.02 l/s occurs through zone 2, which, at the same time is characterized by the largest infiltration area. Zone 3 trenches have the second highest rate of infiltration of surface water, with 65.01 l/s.

The most important outcome of the study is that approximately 99.5% of the surface water diverted from Brenta river is expected to be recharged through zones 1 and 3. Although zone 2 has highest surface area, only 0.5% water infiltration is calculated to occur through this zone. This conversely means that if the infiltration site was reduced to zones 1 and 3 and a loss of infiltration capacity of 0.5% is accepted, the size of the MAR site could theoretically be reduced by 77.9% and be used for other purposes, e.g. agriculture.

### 3.5. Economic analysis of Schiavon FIA

Fig. 6 a & b provide an overview of the capital, annual O&M cost, and levelized cost of Schiavon FIA. The expenses were estimated based on the information obtained for the establishment of 1 ha FIA initiated by Veneto Agriculture within AQUOR project (De Carli 2015). The adaptive site investigation cost was determined following the expert consultation at the Helmholtz Centre for Environmental Research-UFZ Leipzig. The cost parameters in LCUs were considered for the year 2009 when the

MAR site was established. Later it was multiplied with a GDP deflator of 1.15 and an exchange rate of 1.07 to express the standardized cost in US \$ for 2022. Detailed information on the cost analysis can be found in Table S3.

The costs associated with establishing an FIA of 1 ha, including capital, O&M expenses in 2022 is 117,221.14 US\$. From Fig. 6a, it can be observed that the annual O&M cost of Schiavon FIA represent only a small fraction (3.5%) of the capital cost. According to the estimated infiltration value, infiltrating surface water through the initial layout of FIA has a capital cost per  $m^3$  of 0.036 US\$ and a levelized cost of 0.003 US\$ (Fig. 6b).

The standardized land acquisition cost for arable land in 2022 is 79,910 US\$ per ha which constitutes approximately 68.2% of the declared investment cost, showing that land acquisition cost is one of the important factors in determining MAR scheme cost when it is not obtained free. As 22.1% of the FIA is suitable for surface water recharge in the investigated FIA site, land cost will be reduced to 17,660 US\$. The adaptive site investigation cost is 8.57 times higher than the traditional investigation approach. Despite the increased investigation cost, it will lead to 59.1% reduction in levelized cost per  $m^3$  of estimated recharged water.

## 4. Discussion

The site characterization employed an EMI survey and DP profiling as across-scale investigation methods to enhance site delineation. The

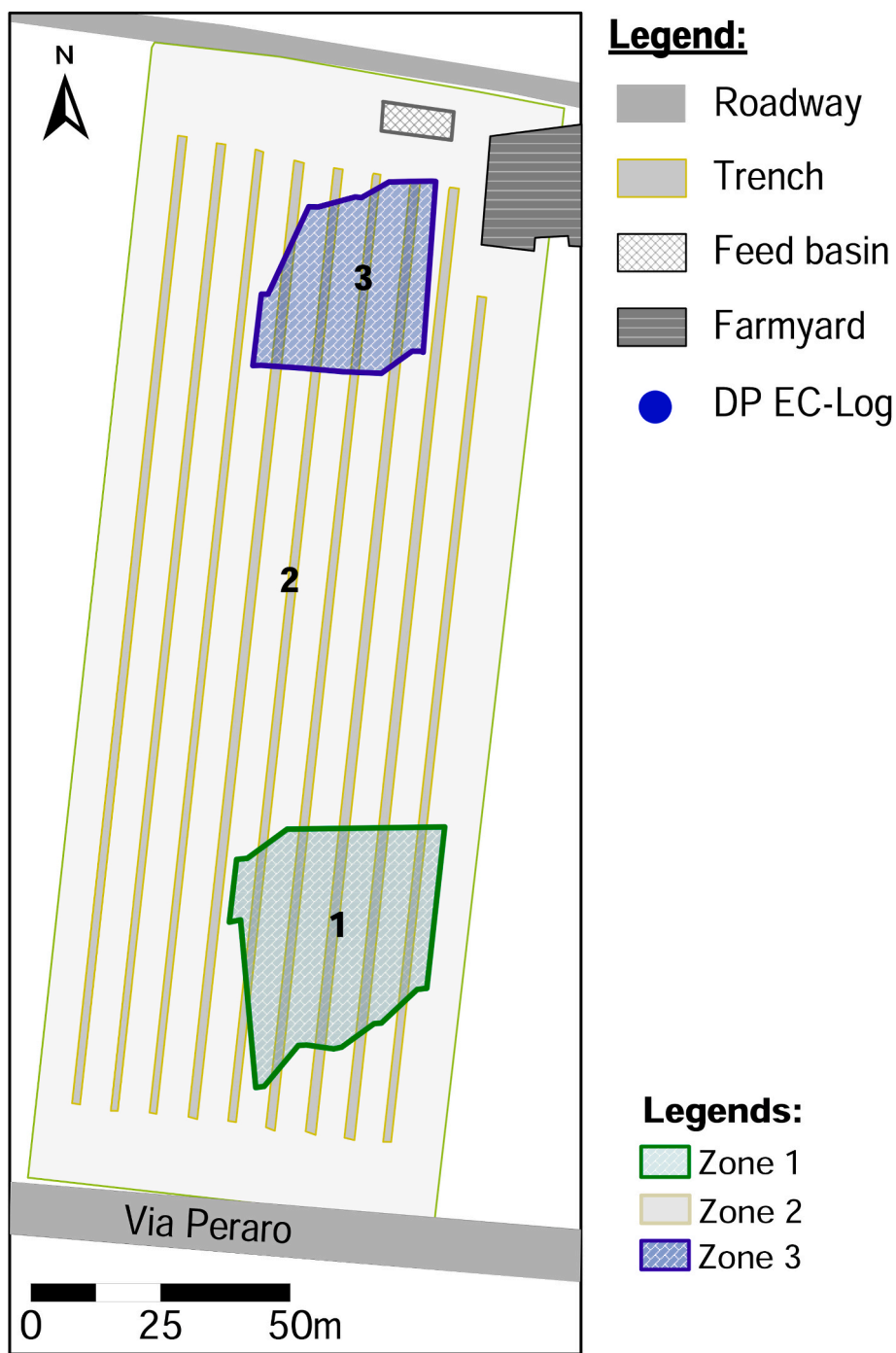


Fig. 5. Three zones with different infiltration characteristics distinguished using EMI and DP techniques.

**Table 1**  
Estimated infiltration rates of three zones identified from the EMI survey and DP techniques.

Zones	Surface area of trenches (m <sup>2</sup> )	Calculated maximum infiltration rates (l/sec)
Zone 1	148.26	124.58
Zone 2	887.98	1.02
Zone 3	103.90	65.01
Total	1140.14	190.61

identified zones were subsequently parameterized using laboratory analysis on the obtained samples. While EMI and DP measurements bear several advantages over traditional site investigation approaches (see section 2.2 and 2.2.2) they are also associated with limitations. For both approaches this includes the measurement of EC<sub>a</sub> and EC which serve only as an indicator for changes in the fine-grained content. In addition, EC<sub>a</sub> provides only a bulk EC value over the support volume during one measurement but no information of the vertical distribution of EC. Hence, DP vertical profiling was applied. The combination of EMI and DP profiling generally provided complementary consistent subsurface information. An exemption was found at probing location EC 06 where the EMI survey indicated comparably high EC<sub>a</sub> values while EC values obtained from DP profiling were comparably low. During the EMI



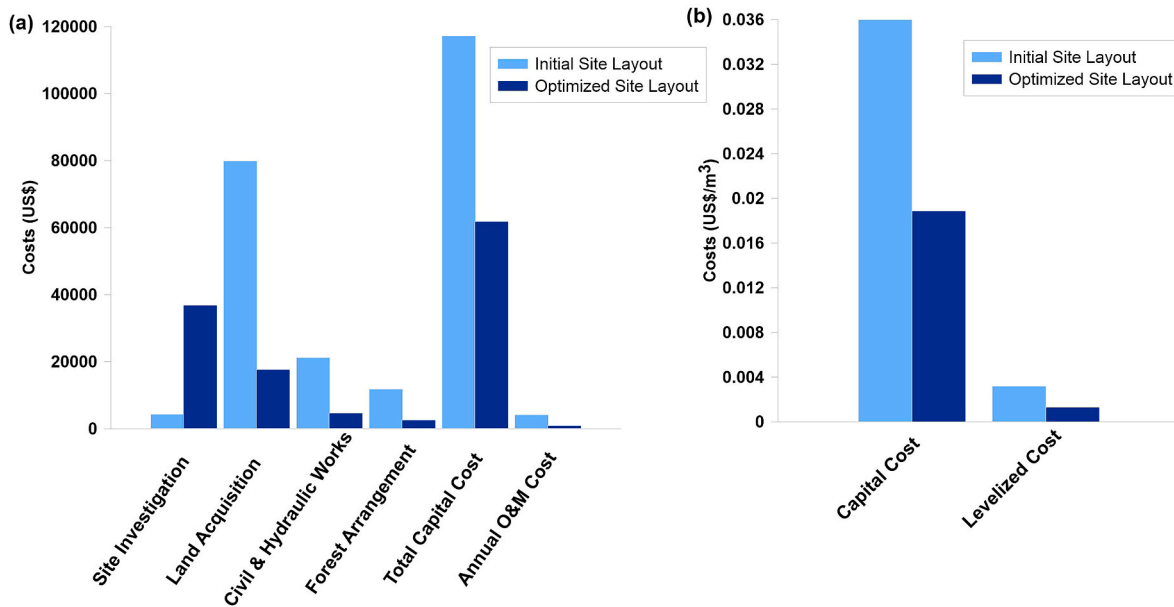


**Fig. 6.** (a) Site investigation, land acquisition, civil & hydraulic works, forest arrangement, capital and annual O&M cost (b) Capital and levelized cost per  $\text{m}^3$  of recharged water for initial and optimized site layout of Schiavon FIA scheme.

measurement, surface water was present in that part of the test site and it is assumed that it influenced the results by producing the encountered high  $\text{EC}_a$  values. Since water was standing in the trenches we constitute the infiltration capacity of this area to be low. Hence, we attributed EC 06 to be part of the low conductive and low infiltration zone despite low EC values.

The generally low measured EC values at EC 01 were already pointed out in the results section. EC load tests were performed before and after each DP EC profile, which confirms that the used equipment worked properly. The most likely reason for low EC values is an insufficient electrical coupling of the DP probe to the soil under dry conditions, indicating the presence of dry non-cohesive sediments. Our investigation also revealed individual discrepancies between the DP measured EC and the grain size analysis result. At EC 01, the difference between the grain size composition change and variation in EC values over two consecutive depth intervals (0.15–0.25 m and 0.4–0.55 m) is noticeable. The probable reason for this mismatch may be the insufficient electrical coupling of the DP EC probe in shallow depths and the remaining inaccuracy regarding the exact soil sampling depth and sample disturbance.

The delineation of zones with different infiltration behavior was primarily based on the results of the EMI survey. Our conceptual site model assumed the delineated individual zones to be composed of similar soil properties. Despite the recognized heterogeneity of the deposits within the Schiavon FIA, our focus was on characterizing zones based on their common property, in this case infiltration rate. Moreover, conducting extensive DP investigations to further characterize the low infiltration zone would not be financially feasible. Achieving an optimal balance between enhancing data availability and deriving substantial benefits from these efforts is essential. The approach adopted not only provides a reliable data foundation but also makes strategic use of tools to maximize information gain. Additionally, even small-scale variations and slight increases in hydraulic conductivity have little effect, as the infiltration rate of zone 2 is approximately two orders of magnitude lower than that of zones 1 and 3. Overall, the investigation approach proved suitable for unraveling the spatial variability in the distribution of  $K_s$  and infiltration rates across the MAR site.

A limitation in this study was encountered in the measurement of  $K_s$  as the most important parameter to determine infiltration rates. The constant head permeameter is operated using a small sample of  $250 \text{ cm}^3$

under controlled conditions with one-dimensional flow. The laboratory measurement hence always depends on the representativeness of the sample and avoidance of sample disturbance, especially under non-isotropic soil conditions. While we aimed to ensure representativity of the samples with the chosen approach, the disturbance of the samples was, however, unavoidable in this case due to soil compaction during sampling and minor core loss at different depth intervals. In-situ measurements of  $K_s$  with a larger sample volume would be preferable but could not be realized in the field as the work was performed in the unsaturated zone above the groundwater table, leaving only laboratory analyses.

The infiltration rate for the optimized MAR layout was calculated to be  $190.61 \text{ l/s}$ . As this reflects a theoretical maximum infiltration for the present trench geometry under constant operation with a water height of 40 cm in the trenches, it is not surprising that the actual monitored hydrologic performance of the site from May 2011 to May 2014 was with  $25.4 \text{ l/s}$  significantly lower (see Mastrocicco et al., 2015 for monitored operation data). Observed infiltration rates were determined using mass balance analysis and point specific temperature measurements. Also, the system was not performing at its maximum capacity (Mastrocicco et al., 2015).

Ross and Hasnain (2018) presented MAR scheme cost in different countries and the levelized cost of the MAR scheme varied between  $0.07 \text{ US\$}$  and  $2.67 \text{ US\$ per m}^3$ . Ross (2022), reported in an overview of 24 MAR schemes costs in a wide range from  $0.007 \text{ US\$}$  to  $5.252 \text{ US\$ per m}^3$ . These studies show that several factors, including the types of MAR techniques, water source, treatment of water, the scale of the MAR infrastructure, scheme usage frequency and operation period, MAR scheme life expectancy, and hydrogeological setting of the site influence the cost of MAR schemes besides capital costs. The expenses associated with constructing the surface spreading MAR schemes and land acquisition, however, are significant elements that add to the overall expenses of these schemes (Ross and Hasnain, 2018). It is important to note that the uncertainty involved in estimating the infiltration rate in our study impacts the cost estimation of the infiltrated water. Although the levelized cost of the Schiavon FIA in both scenarios is low if compared to the above-mentioned studies, the objective of this research was not to compare these costs with other studies.

MAR assessments are often conducted on a regional scale because understanding regional hydrogeology is crucial for effective site

positioning. A regional assessment is, however, not part of our work as we focus on the site-specific estimation of spatially resolved infiltration rates and cost analysis for MAR infrastructures.

## 5. Conclusion

Worldwide there is an increasing need for MAR sites, as declining groundwater supply and growing demand need to be balanced. It is imperative to have a realistic understanding and conceptualization of the subsurface structure along with the financial and economic characteristics of MAR to assess the performance and feasibility of MAR schemes. This study provides a promising approach for future MAR planning using surface spreading methods by providing an example to engineers, water planners, researchers and policymakers on how to efficiently characterize MAR sites and predict infiltration rates, followed by a preliminary assessment of the cost incurred by the MAR infrastructure. The adaptive investigation approach overcomes data scarcity and uncertainties often associated with conventional, point-based investigation methods with limited flexibility. With this, we contribute to the technical and economic optimization of MAR systems and thereby aim to foster their uptake.

## Financial support

This research work is supported by the European Union's Horizon 2020 research and innovation programme under the Marie Skłodowska-Curie grant agreement no. 814066 (Managed Aquifer Recharge Solutions Training Network - MARSoluT).

## CRedit authorship contribution statement

**Rebecca Sultana:** Conceptualization, Formal analysis, Methodology, Writing – review & editing, Writing – original draft. **Ulrike Werban:** Writing – review & editing, Conceptualization, Methodology, Project administration, Supervision. **Marco Pohle:** Data curation, Investigation, Writing – review & editing. **Thomas Vienken:** Project administration, Supervision, Writing – review & editing, Conceptualization, Methodology.

## Declaration of competing interest

The authors declare that they have no known competing financial interests or personal relationships that could have appeared to influence the work reported in this paper.

## Data availability

Data will be made available on request.

## Acknowledgement

We would like to express our gratitude towards our colleagues Helko Kotas, Andreas Schossland, and Manuel Kreck for their continuous support during the MAR site investigation.

## Appendix A. Supplementary data

Supplementary data to this article can be found online at <https://doi.org/10.1016/j.gsd.2024.101169>.

## References

ASR Systems, 2006. Survey of Aquifer Storage and Recovery Capital and Operating Costs in Florida. ASR Systems, Gainesville.  
 Barquero, F., Fichtner, T., Stefan, C., 2019. Methods of in situ assessment of infiltration rate reduction in groundwater recharge basins. *Water* 11 (784). <https://doi.org/10.3390/w11040784>.

Becker, M.W., Bauer, B., Hutchinson, A., 2013. Measuring artificial recharge with fiber optic distributed temperature sensing. *Groundwater* 51, 670–678. <https://doi.org/10.1111/j.1745-6584.2012.01006.x>.  
 Binley, A., Hubbard, S.S., Huisman, J.A., Revil, A., Robinson, D.A., Singha, K., Slater, L.D., 2015. The emergence of hydrogeophysics for improved understanding of subsurface processes over multiple scales. *Water Resour. Res.* 51, 3837–3866. <https://doi.org/10.1002/2015WR017016>.  
 Bouwer, H., 2002. Artificial recharge of groundwater: hydrogeology and engineering. *Hydrogeol. J.* 10, 121–142. <https://doi.org/10.1007/s10040-001-0182-4>.  
 Butler, J.J., 2002. A simple correction for slug tests in small-diameter wells. *Ground Water* 40, 303–307. <https://doi.org/10.1111/j.1745-6584.2002.tb02658.x>.  
 Callegary, J.B., Ferré, T.P.A., Groom, R.W., 2012. Three-dimensional sensitivity distribution and sample volume of low-induction-number electromagnetic-induction instruments. *Soil Sci. Soc. Am. J.* 76, 85–91. <https://doi.org/10.2136/sssaj2011.0003>.  
 Casanova, J., Devau, N., Pettenati, M., 2016. Managed aquifer recharge: an overview of issues and options. In: Jakeman, A.J., Barreteau, O., Hunt, R.J., Rinaudo, J.-D., Ross, A. (Eds.), *Integrated Groundwater Management: Concepts, Approaches and Challenges*. Springer International Publishing, Cham, pp. 413–434. [https://doi.org/10.1007/978-3-319-23576-9\\_16](https://doi.org/10.1007/978-3-319-23576-9_16).  
 De Carli, A., 2015. Deliverable A.5. Analisi economico-finanziaria delle soluzioni tecniche per il riequilibrio delle falde nell'ambito del progetto AQUOR.  
 De Marsily, Gh, Delay, F., Gonçalves, J., Renard, Ph, Teles, V., Violette, S., 2005. Dealing with spatial heterogeneity. *Hydrogeol. J.* 13, 161–183. <https://doi.org/10.1007/s10040-004-0432-3>.  
 Dietrich, P., Leven, C., 2006. Direct push-technologies. In: Kirsch, R. (Ed.), *Groundwater Geophysics: A Tool for Hydrogeology*. Springer, Berlin, Heidelberg, pp. 321–340. [https://doi.org/10.1007/3-540-29387-6\\_11](https://doi.org/10.1007/3-540-29387-6_11).  
 Dillon, P., Pavelic, P., Page, D., Beringen, H., Ward, J., 2009. *Managed Aquifer Recharge: an Introduction*.  
 Doolittle, J.A., Brevik, E.C., 2014. The use of electromagnetic induction techniques in soils studies. *Geoderma* 223–225, 33–45. <https://doi.org/10.1016/j.geoderma.2014.01.027>.  
 EPA, 1997. Expedited Site Assessment Tools for Underground Storage Tank Sites - A Guideline for Regulators. Office of Solid Waste and Emergency Response. U.S. Government Printing Office, Pittsburgh.  
 Filippi, E., Marcala, V., Ferri, M., Cisotto, A., Vienken, T., Kofakis, P., 2016. Deliverable 7.1. MAR through forested infiltration in the river Brenta Catchment, Vicenza, Italy, 46 pp. FP7 MARSOL (Demonstrating Managed Aquifer Recharge as a Solution to Water Scarcity and Drought).  
 Gale, I., Neumann, I., Calow, R., Moench, M., 2002. The effectiveness of artificial recharge of groundwater: a review. Nottingham. British Geological Survey, UK, p. 60. <https://nora.nrc.ac.uk/id/eprint/527471>.  
 Giordano, M., 2009. Global groundwater? Issues and solutions. *Annu. Rev. Environ. Resour.* 34, 153–178. <https://doi.org/10.1146/annurev.enviro.030308.100251>.  
 Giordano, M., Villholth, K.G., 2007. *The Agricultural Groundwater Revolution: Opportunities and Threats to Development*. CAB International.  
 Halysia, O., Vracholi, M., Janik, K., Sitek, S., Wojtal, G., Imig, A., Rein, A., Sauer, J., 2022. Assessing economic feasibility of managed aquifer recharge schemes: evidence from cost-benefit analysis in Poland. *Water Resour. Manag.* 36, 5241–5258. <https://doi.org/10.1007/s11269-022-03303-0>.  
 Hossain, MdI., Bari, MdN., Miah, S.U., Kafy, A.-A., Nasher, N.M.R., 2021. Application of modified managed aquifer recharge model for groundwater management in drought-prone water-stressed Barind Tract, Bangladesh. *Environmental Challenges* 4, 100173.  
 Jakeman, A.J., Barreteau, O., Hunt, R.J., Rinaudo, J.-D., Ross, A., Arshad, M., Hamilton, S., 2016. Integrated groundwater management: an overview of concepts and challenges. In: Jakeman, A.J., Barreteau, O., Hunt, R.J., Rinaudo, J.-D., Ross, A. (Eds.), *Integrated Groundwater Management: Concepts, Approaches and Challenges*. Springer International Publishing, Cham, pp. 3–20. [https://doi.org/10.1007/978-3-319-23576-9\\_1](https://doi.org/10.1007/978-3-319-23576-9_1).  
 Kalbus, E., Reinstorf, F., Schirmer, M., 2006. Measuring methods for groundwater & surface water interactions: a review. *Hydrol. Earth Syst. Sci.* 10, 873–887. <https://doi.org/10.5194/hess-10-873-2006>.  
 Koltermann, C.E., Gorelick, S.M., 1996. Heterogeneity in sedimentary deposits: a review of structure-imitating, process-imitating, and descriptive approaches. *Water Resour. Res.* 32, 2617–2658. <https://doi.org/10.1029/96WR00025>.  
 Maliva, R.G., 2014. Economics of managed aquifer recharge. *Water* 6, 1257–1279. <https://doi.org/10.3390/w6051257>.  
 Maliva, R.G., Guo, W., Missimer, T.M., 2006. Aquifer storage and recovery: recent hydrogeological advances and system performance. *Water Environ. Res.* 78, 2428–2435. <https://doi.org/10.2175/106143006X123102>.  
 Maréchal, J.-C., Bouzit, M., Rinaudo, J.-D., Moiroux, F., Desprats, J.-F., Caballero, Y., 2020. Mapping economic feasibility of managed aquifer recharge. *Water* 12 (680). <https://doi.org/10.3390/w12030680>.  
 Martini, E., Werban, U., Zacharias, S., Pohle, M., Dietrich, P., Wollschläger, U., 2017. Repeated electromagnetic induction measurements for mapping soil moisture at the field scale: validation with data from a wireless soil moisture monitoring network. *Hydrol. Earth Syst. Sci.* 21, 495–513. <https://doi.org/10.5194/hess-21-495-2017>.  
 Mastrocicco, M., Colombani, N., Salemi, E., Boz, B., Gumiero, B., 2015. Managed aquifer recharge via infiltration ditches in short rotation afforested areas. *Ecology* 9, 167–178.  
 Mawer, C., Parsekian, A., Pidlisecky, A., Knight, R., 2016. Characterizing heterogeneity in infiltration rates during managed aquifer recharge. *Ground Water* 54, 818–829. <https://doi.org/10.1111/gwat.12423>.

- McNEILL, J., 1980. Electromagnetic Terrain Conductivity Measurement at Low Induction Numbers. Geonics Ltd., Technical Note TN-6.
- Medina, R., Pham, C., Plumlee, M.H., Hutchinson, A., Becker, M.W., O'Connell, P.J., 2020. Distributed temperature sensing to measure infiltration rates across a groundwater recharge basin. *Groundwater* 58, 913–923. <https://doi.org/10.1111/gwat.13007>.
- METER Group AG, 2016. KSAT operation manual. [http://library.metergroup.com/Mannuals/UMS/KSAT\\_Manual.pdf](http://library.metergroup.com/Mannuals/UMS/KSAT_Manual.pdf).
- Morris, B.L., Lawrence, A.R.L., Chilton, P.J.C., Adams, B., Calow, R.C., Klinck, B.A., 2003. Groundwater and its Susceptibility to Degradation : a Global Assessment of the Problem and Options for Management. United Nations Environment Programme.
- Naik, P.K., Mojica, M., Ahmed, F., Al-Mannai, S., 2017. Storm water injection in Bahrain: pilot studies. *Arabian J. Geosci.* 10 (452) <https://doi.org/10.1007/s12517-017-3232-5>.
- OECD, 2022. Main economic indicators - complete database. Main Econ. Indicat. <https://doi.org/10.1787/data-00052-en>. (Accessed 14 November 2022).
- Piccinini, L., Fabbri, P., Pola, M., 2016. Point dilution tests to calculate groundwater velocity: an example in a porous aquifer in northeast Italy. *Hydrol. Sci. J.* 61, 1512–1523. <https://doi.org/10.1080/02626667.2015.1036756>.
- Racz, A.J., Fisher, A.T., Schmidt, C.M., Lockwood, B.S., Los Huertos, M., 2012. Spatial and temporal infiltration dynamics during managed aquifer recharge. *Ground Water* 50, 562–570. <https://doi.org/10.1111/j.1745-6584.2011.00875.x>.
- Ross, A., 2016. Groundwater Governance in Australia, the European union and the Western USA. In: Jakeman, A.J., Barreteau, O., Hunt, R.J., Rinaudo, J.-D., Ross, A. (Eds.), *Integrated Groundwater Management: Concepts, Approaches and Challenges*. Springer International Publishing, Cham, pp. 145–171. [https://doi.org/10.1007/978-3-319-23576-9\\_6](https://doi.org/10.1007/978-3-319-23576-9_6).
- Ross, A., 2022. Benefits and costs of managed aquifer recharge: further evidence. *Water* 14 (3257). <https://doi.org/10.3390/w14203257>.
- Ross, A., Hasnain, S., 2018. Factors affecting the cost of managed aquifer recharge (MAR) schemes. *Sustain. Water Resour. Manag.* 4, 179–190. <https://doi.org/10.1007/s40899-017-0210-8>.
- Schulmeister, M.K., Butler Jr, J.J., Healey, J.M., Zheng, L., Wysocki, D.A., McCall, G.W., 2003. Direct-push electrical conductivity logging for high-resolution hydrostratigraphic characterization. *Ground Water Monit. Remediation* 23, 52–62. <https://doi.org/10.1111/j.1745-6592.2003.tb00683.x>.
- Sottani, A., Bertoldo, S., Campagnolo, F., Altissimo, L., Gusmaroli, G., Muraro, T., 2014. Esperienze di MAR con sistemi disperdenti a largo diametro: primo bilancio di attività sperimentali nell'alta pianura vicentina (Italia Settentrionale). *Acque Sotterranee*. <https://doi.org/10.7343/AS-082-14-0108>.
- Sprenger, C., Hartog, N., Hernández, M., Vilanova, E., Grützmacher, G., Scheibler, F., Hannappel, S., 2017. Inventory of managed aquifer recharge sites in Europe: historical development, current situation and perspectives. *Hydrogeol. J.* 25, 1909–1922. <https://doi.org/10.1007/s10040-017-1554-8>.
- Swamee, P.K., Mishra, G.C., Chahar, B.R., 2000. Design of minimum seepage loss canal sections. 6. *J. Irrig. and Drain. Engrg. ASCE* 126 (1), 28–32.
- Treasury, H.M.S., 2003. *The Green Book: Appraisal and Evaluation in Central Government*. TSO, London.
- Utom, A.U., Werban, U., Leven, C., Müller, C., Dietrich, P., 2019. Adaptive observation-based subsurface conceptual site modeling framework combining interdisciplinary methodologies: a case study on advancing the understanding of a groundwater nitrate plume occurrence. *Environ. Sci. Pollut. Res.* 26, 15754–15766. <https://doi.org/10.1007/s11356-019-05048-7>.
- Vienken, T., Dietrich, P., 2011. Field evaluation of methods for determining hydraulic conductivity from grain size data. *J. Hydrol.* 400, 58–71. <https://doi.org/10.1016/j.jhydrol.2011.01.022>.
- Vienken, T., Leven, C., Dietrich, P., 2012. Use of CPT and other direct push methods for (hydro-) stratigraphic aquifer characterization — a field study. *Can. Geotech. J.* 49 (2), 197–206. <https://doi.org/10.1139/t11-094>.
- Vienken, T., Huber, E., Kreck, M., Huggenberger, P., Dietrich, P., 2017. How to chase a tracer – combining conventional salt tracer testing and direct push electrical conductivity profiling for enhanced aquifer characterization. *Adv. Water Resour.* 99, 60–66.
- Vitharana, U.W.A., Van Meirvenne, M., Cockx, L., Bourgeois, J., 2006. Identifying potential management zones in a layered soil using several sources of ancillary information. *Soil Use Manag.* 22, 405–413. <https://doi.org/10.1111/j.1475-2743.2006.00052.x>.
- von Suchodoletz, H., Pohle, M., Khosravichenar, A., Ulrich, M., Hein, M., Tinapp, C., Schultz, J., Ballasus, H., Veit, U., Ettel, P., Werther, L., Zielhofer, C., Werban, U., 2022. The fluvial architecture of buried floodplain sediments of the Weiße Elster River (Germany) revealed by a novel method combination of drill cores with two-dimensional and spatially resolved geophysical measurements. *Earth Surf. Process. Landforms* 47 (4), 955–976. <https://doi.org/10.1002/esp.5296>.